

# Characterisation of the noise affecting magnetic tweezers' measures

Author: Víctor Sáez Ros

*Facultat de Física, Universitat de Barcelona, Diagonal 645, 08028 Barcelona, Spain.*

Advisor: Maria Mañosas

**Abstract:** Magnetic tweezers are used to study and manipulate biomolecules by using a microscope and a CCD camera to track the position of micron-sized magnetic beads inside a microfluidic chamber. In these experiments we can attach the molecule of interest to a bead, and adjust the position of a pair of magnets placed above the chamber to apply different forces to the tethered molecule and track the molecule extension in real time. The resolution of these measurements are mainly affected by three sources of noise: the tracking noise, the Brownian motion noise and the low-frequency noise. Here we characterised these types of noise. We found that the tracking noise increases with the frequency at which the camera track as expected for a Poissonian uncorrelated noise. For the Brownian case, the noise increased with the length of the tethered molecule and decreases with the force applied. The dependencies found could be reproduced with a simple description of an inverted overdamped pendulum and using standard polymer models for the molecule elasticity. The low-frequency noise was present in all the experiments and could be corrected by subtracting the average position of fixed beads inside the chamber.

## I. INTRODUCTION

Magnetic tweezers (MT) are a really good set up that in the last years have been used in various experiments in the biophysics branch [1, 2]. Mostly this experiments consist in manipulating biomolecules, such as nucleic acids (DNA and RNA) and proteins. MT allow manipulating individual molecules by applying forces on the scale of the pN and studying their mechanical properties, their folding and their binding kinetics [1]. The characterisation of these biomolecular processes rely on measurements that have errors from different sources. These errors limit the resolution of our measurements. In this project we want to characterise the different types of noise to investigate how the different elements limit the final resolution.

With MT we typically attach a micron-sized bead to the molecule of interest and measure the bead's position with video-microscopy. The position measurement reports the molecule length that is used as a reaction coordinate to study the process of interest (i.e folding). The micron-sized beads (attached to the molecule of interest) are flowed into a microfluidic chamber, that is illuminated by a LED and are imaged using an inverted microscope and a CCD camera. The set up uses parallel illumination, that create diffraction images of the beads consisting on a set of rings. These rings allow to perform 3D tracking of the position of the beads.

There are mainly three sources of noise in the experimental system [3] that limit our resolution: the tracking noise in the determination of the bead position, the low-frequency mechanical drift, and the thermal noise arising from the Brownian fluctuations of the DNA-tethered bead. The first is limited by the number of photons that arrive to the camera and the algorithm to extract position measurements from image analysis. In order to investigate this noise we can vary the frequency  $f_s$  at

which the camera works, changing the amount of photons  $N$  registered by the camera:  $f_s \sim 1/N$  at fix illumination. The second source of noise is due to the way the bead-tethered-molecule move in the fluid environment due to thermal fluctuations, the so called Brownian motion. This motion governs the micron/nanometer-size world inside cells. Here we investigate the effect of the Brownian noise studying molecules of different lengths and under different applied forces using both double-stranded DNA (dsDNA) and single-stranded DNA (ssDNA). Finally, the last source is the low-frequency drift due to mechanical vibrations and temperature changes, which is less important as the instrumental setup is better isolated. In the following we study the different experimental noises and investigate how we can decrease them to achieve the best resolution. To do so, we measure the variance of the bead position signal to determine the amplitude of the noise in the real space and also perform measurements of the power spectrum in the frequency domain to obtain information of the type of noise.

## II. SETUP AND METHODS:

### A. Set up

The MT set up is presented in Fig.(1). It consists in a small pair of magnets that create a large magnetic field gradient located on the top of a microfluidic chamber where super-paramagnetic beads are introduced. The chamber is illuminated with a red LED which power intensity can be tuned. Below the chamber we have an inverted microscope. The image of the microscope is registered by the CCD camera that is connected to the computer, where we have a software designed to track the beads. The camera can work with different acquisition frequencies  $f_s$  reaching a maximum frequency of

600Hz. Also, via this software we were able to change the position of the magnets, changing the force applied to the beads. This system was used to record the position of beads attached to the glass surface of the microfluidic chamber with or without a DNA tether.

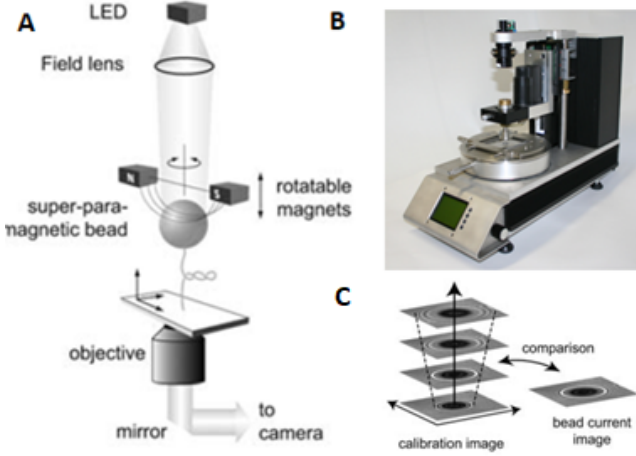


FIG. 1: (A) Schematic representation of the MT with a ssDNA chain tethered to a magnetic bead. The ssDNA has a region of complementarity that can form a double helix structure closed by a loop, called a hairpin structure. (B) Photo of the MT. (C) Bead's diffraction rings at different  $z$  position. Their size depends on  $z$  linearly.

### B. Assays for measuring the tracking noise

To study the tracking noise we performed measurements with beads melted to the microfluidic chamber (without molecule) to minimise the effect of the Brownian motion. In order to achieve that, we heated a slide with a solution that only contained beads for 5 minutes at 100 °C. With that, we evaporated most of the fluid in the slide and the beads melted to the glass surface. Then, we put the slide on top of the microscope objective and tracked the 3D position of the beads. We performed measurements at different frequencies  $f_s$  ranging from 30 Hz to 300 Hz at constant illumination. For each one of the frequencies we tracked the  $x$ ,  $y$  and  $z$  position of the same 24 beads for 50 seconds and measure the variance and the power spectrum. In order to avoid drift effects we decided to work with small time-window (5 seconds window). Furthermore, for each bead we subtracted the average position of all the other beads. These differential measurements are expected to strongly decrease the low-frequency noise because the effects of thermal and mechanical vibrations are present in all beads simultaneously. We computed the signal-to-noise ratio (SNR) to compare the level of noise given by the variance  $\sigma^2$  to the intensity of the signal  $I$ :  $SNR = \frac{\sigma}{I}$  [3]. For the tracking noise the signal is Poissonian distributed due to the arrival of photons to the photodetector and so both the

intensity and the variance are proportional to the number of photons  $N$  ( $\sigma^2 \propto N$  and  $I \propto N$ ). Consequently:

$$SNR = \frac{\sigma_{x,y,z}}{I} \propto \frac{1}{\sqrt{N}} \propto \sqrt{f_s} \quad (1)$$

Another way of characterising the noise is to compute the power spectrum (PSD) of the signal (in our experiments  $x(t)$ ,  $y(t)$  and  $z(t)$ ), which allows to perform a spectral analysis. The shape of the PSD gives information of the type of noise: for Poissonian noise the power spectrum is expected to be flat, since it is a totally uncorrelated noise.

### C. Assays for measuring the Brownian noise

We investigated how the Brownian motion depends on the characteristic of the molecule attached (length or stiffness) and the force applied to the molecule. In order to study the force effect we used a long dsDNA molecule of 48.000 base-pairs (bp) tethered to the magnetic bead (Fig. 3B)). The DNA molecule was attached on one end to the magnetic bead, and on the other end to the surface of the microfluidic chamber, via biotin-streptavidin and digoxigenin-antidigoxigenin interactions. The force applied to the bead (and so to the DNA molecule) was controlled by the position of the magnets placed above the chamber. We measured the  $x - y - z$  bead localisation for several beads when applying eight different forces, from  $\sim 5$  pN to  $\sim 20$  pN. We measured the amplitude of the fluctuations, computing the variance of the signal and also computed the power spectrum. For this experiment, we analysed the signal as if the beads were inverted pendulums with length  $l$  equal to the length of the DNA molecule pulled by a magnetic force  $F$ . Like that, when the bead moves away from the equilibrium position a restoring force is generated, that can be seen as a spring of stiffness  $k$ . For each degree of freedom,  $x, y, z$ :  $1/2k_B T = 1/2k_{x,y,z} \langle \sigma_{(x,y,z)}^2 \rangle$  is verified (equipartition theorem). Therefore the amplitude of the fluctuations are related to the stiffness as:

$$\langle \sigma_{x,y,z}^2 \rangle = \frac{k_B T}{k_{x,y,z}} \quad (2)$$

For high enough forces (small fluctuations) the stiffness in the  $x$  and  $y$  directions are directly related to the force as  $k_{x,y} = \frac{F}{l}$ . This is typically the way in which the force is measured in the experiments, which requires the previous determination of the stiffness. In the experimental conditions, the movement of the bead is overdamped and can be described with a Langevin dynamics [4]:

$$k_x x(t) + \gamma \eta r \frac{\delta x}{\delta t} = F_L(t), \quad (3)$$

where  $\gamma$  is a constant depending on the geometry ( $6\pi$  for a sphere, like our beads),  $\eta$  corresponds to the viscosity of the medium ( $\eta_{water} = 10^{-3} Pa \times s$ ),  $r$  is the radius of the bead ( $r = 1\mu m$ ) and  $F_L$  is the Langevin force. To

obtain the stiffness experimentally, we compute the PSD of the signal  $|\tilde{x}(f)|^2$  (we did not work with the  $y$  position because it is equivalent to  $x$ ), that is expected to follow a Lorentzian function with the form (computed from the fourier transform of Eq.(3)):

$$|\tilde{x}(f)|^2 = \frac{4\gamma\eta r k_B T}{k_x^2} \frac{1}{1 + (f/f_c)^2} \quad (4)$$

where the corner frequency  $f_c$  is given by :

$$f_c \equiv \frac{k_x}{2\pi\gamma\eta r} = \frac{F}{12\pi^2\eta r l} \quad (5)$$

The frequency  $f_c$  gives the characteristic response time of the system  $\tau_b = (2\pi f_c)^{-1}$ . In order to measure it correctly, we need a small signal sampling period  $t_s \equiv 1/f_s$ , relative to the response time, typically  $f_s > 4f_c$ . We also need to take data for a long time, so that  $T \gg \tau_b$ . By fitting the experimental power spectrum data to a Lorentzian function we measure  $f_c$  and find the stiffness via Eq.(5), which allows us to study the noise level as a function of the stiffness.

The determination of  $f_c$  from the power spectrum analysis for  $x$  and  $y$  worked fine. But it did not for the  $z$  direction where corner frequencies were higher. Therefore, to estimate  $k_z$  we used an alternative method. We measured the force versus extension ( $z$ ),  $F(z)$  and compute  $k_z = \partial F / \partial z$ . The elasticity  $F(z)$  for dsDNA is well reproduced by the worm-like-chain model (WLC) that describes the DNA molecule as a semi-flexible polymer as: [5].

$$F(z) = \frac{k_B T}{P} \left[ \frac{1}{4} \left( 1 - \frac{z}{L} \right)^{-2} - \frac{1}{4} + \frac{z}{L} \right] \quad (6)$$

where  $P$  is the persistence length, defined as the length at which the tangent vector decorrelates, and  $L$  the contour length, corresponding to the maximum length of the totally extended polymer. Our data  $F(z)$  could be fitted to this model (Eq.(6)) and from that we could estimate  $k_z$  and investigate the noise as a function of the stiffness.

In order to study the effect of the tether length, instead of using a dsDNA molecule we used a ssDNA molecule, and we tethered it to the bead and the microfluidic chamber using the same approach than in the previous experiment. This type of molecules are designed to have a region of complementarity that hybridise forming a dsDNA helix closed by a loop. The structure is called a hairpin, as seen in Fig.(5B). Our ssDNA molecule had approximately 2900 nucleotides (nts) when the hairpin is opened. To study the lenght-dependence of the noise we opened the hairpin at different lengths and study the  $z$ -fluctuations at a constant reference force (around 10pN). To do that, we used oligonucleotides (oligos), which are small pieces of DNA that have the specific sequence to attach to a determined position along the ssDNA [6]. Initially, we applied a large force to the DNA hairpin so

that the hairpin unfolds by opening all the base-pairs. We next introduced the oligo that hybridises to a specific region of the ssDNA sequence. We next decreased the force to the reference value ( $\sim 10$ pN). At this force the hairpin reformed until the position where the oligo was hybridized. The oligos prevented the molecule to zip back completely, so it was left with a number  $n$  of nts open ( $n$  going from 100 to 2900). We introduced into the microfluidic chamber the oligos one by one, starting from the ones that left the molecule more closed. The last oligo was placed in the loop of the hairpin, so the molecule was opened completely. To study the  $z$  fluctuations, we first calculated the power spectrum for the signal obtained with all ssDNA extensions. Since the variance  $\langle \sigma_z^2 \rangle = \frac{k_B T}{k_z}$  and  $k_z$  are inversely proportional to the contour length  $L$  of the molecule, which increases linearly with the number  $n$  of open ssDNA nts, we find the following relation:

$$\langle \sigma_z^2 \rangle \propto 1/k_z \propto n. \quad (7)$$

### III. RESULTS:

#### A. Tracking noise

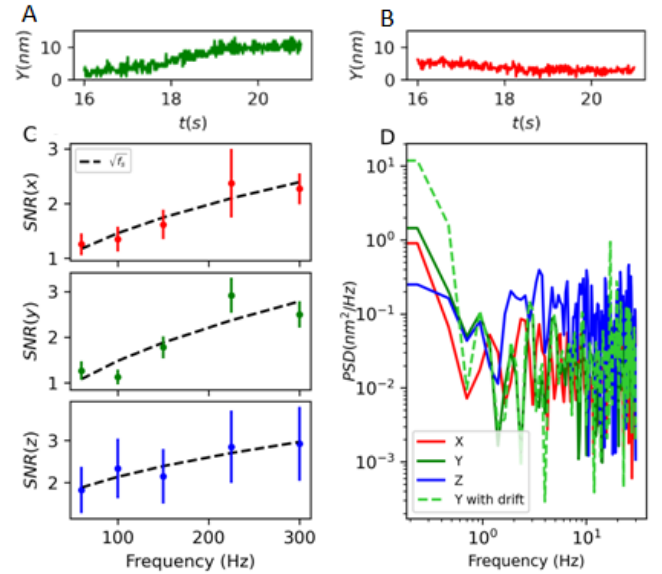


FIG. 2: (A) Tracking of the  $y$  position for one bead in a 5 second window. (B) Same as A but correcting the drift by subtracting several beads. (C) SNR of the position of melted beads in the axis  $x$ ,  $y$  and  $z$  as a function of the Frequency of the camera  $f_s$ . (D) Power spectrum for the  $x$ ,  $y$ ,  $z$  position of the bead. Results shown are obtained from differential measurements between several beads to decrease drift. For the  $y$  results we also show the raw data (without differential measurements) for comparison in a discontinuous line.

The results obtained for the tracking noise are presented in Fig.(2). As we expected, the SNR of the position of the beads increases at a rate proportional to  $\sqrt{f_s}$ , as expected, Eq.(1). Note that the error associated to the  $z$  axis is way bigger than that for the  $x$  and  $y$  axis. This is clearly caused by the different methods to obtain the tracking for the  $z$  axis and the  $x$  and  $y$  axis. While the  $x$  and  $y$  positions are obtained from the localisation of the center of the diffraction rings, the  $z$  position requires an extrapolation method that relates the  $z$  position with the shape of the rings. This later method has a larger intrinsic error (Fig.(1C)).

The measured power spectrum is flat as expected for a Poissonian shot noise. At low frequencies the values for the power spectrum increases due to the low-frequency drift. This is improved by averaging several beads (see comparison between continuous and dashed green lines) but not totally suppressed (at the lowest frequencies that PSD values are always larger)

### B. Brownian noise

In order to study the effect of the Brownian noise we have measured the position of tethered beads as a function of the force applied and the tether length. For the force study we use a long dsDNA molecule (DNA from  $\lambda$  phage of 48 Kbp), and study the  $x$  and  $z$  axis separately, which differ because the stiffness in  $z$  is different than the stiffness in the horizontal plane (the  $y$  axis is analogous to the  $x$  axis). As shown in Fig.(3A) the power spectrum of the  $x$  signal follows a Lorentzian function with PSD values at low frequencies increasing as the force decreases. This is a consequence that the amplitude of fluctuations decreases with force. From fitting the power spectrum to a

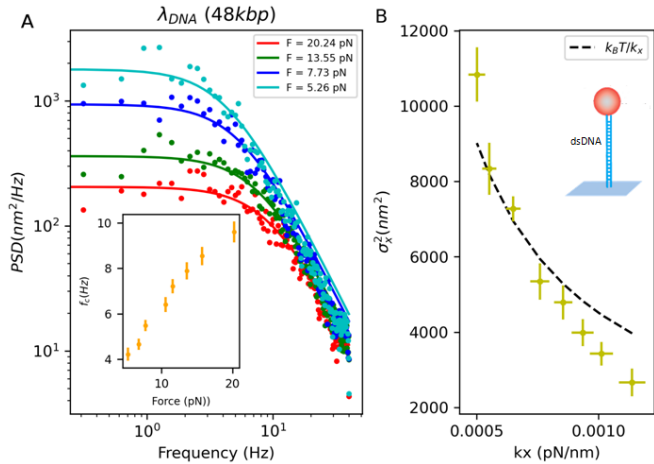


FIG. 3: (A) Power spectrum of the  $x$  position for four of the different forces applied to the beads. Also an inset with the  $f_c$  for each force. (B) Variance in  $x$  depending and a schematic representation of dsDNA attached to a bead.

Lorentzian function we could find  $f_c$  for the forces studied

(see inset). From  $f_c(F)$  values we obtained  $k_x(F)$  using Eq.(5). Then, we represented the measured variance as a function of  $k_x(F)$ , Fig.(3B), and show that the measured dependence approaches to the  $k_B T / k_x(F)$  expected value (Eq.(2)).

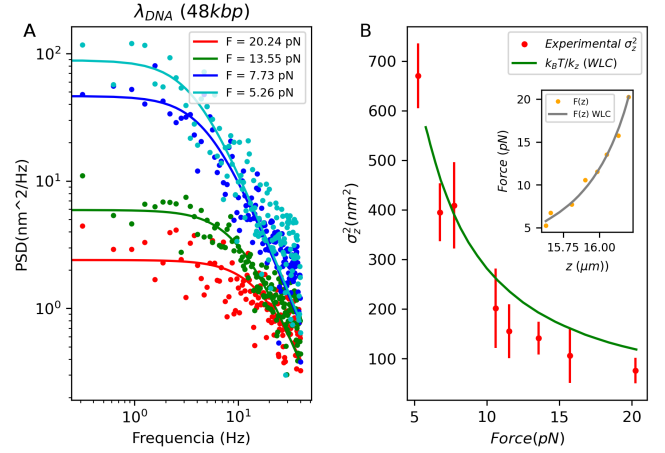


FIG. 4: (A) Power spectrum of the  $z$  position for four of the different forces applied to the beads. (B) Comparison between the curve of the WLC model and the experimental results. Also an inset of the force depending on the extension of the molecule and the curve obtained by the WLC model.

In Fig.(4A) we show the power spectrum of the  $z$  position for the different forces. As compared with the  $x$  results (Fig.(3)), the PSD values for  $z$  are lower (meaning that the amplitude of the fluctuations are lower), and the power spectra are way more flat. The later is due to the fact that  $f_c$  values are larger for the  $z$  position. Indeed  $f_c$  for  $z$  cannot be obtained from the fits, because the condition  $f_c < 4f_s$  is not verified. However, we can estimate  $k_z$  using the force-extension measurements  $F(z)$ . The force-extension curve  $F(z)$  can be fitted to the WLC model (as seen in the inset of Fig.(4A)) and the  $k_z$  obtained computing the derivative. Doing this analysis the measured variance is compared to the expected value  $k_B T / k_z$ , Fig.(4A)).

Finally, to investigate how the Brownian noise is affected by the length of the DNA tether we performed experiments with a ssDNA molecule whose length can be controlled with the usage of different short oligos (see Methods). With this technique we explored tether lengths from 100 to 2900 nts. The power spectrum of the  $z$  position, Fig.(5A), show how the level of noise (at low frequencies) increases with the number of open nts ( $n$ ). The PSD results have been fitted to Lorentzian functions, even that the shorter tethers have mainly a flat spectrum. This is a consequence of the fact that  $f_c$  is very large for short molecules, and therefore it cannot be observed in the PSD results, at the experimental  $f_s$ . However, as we know that the stiffness  $k_z$  is inversally proportional to  $n$ , we expect the amplitude of fluctuations to increase with  $n$  (Eq.(7)).



As a comparison we show the PSD of the tracking noise

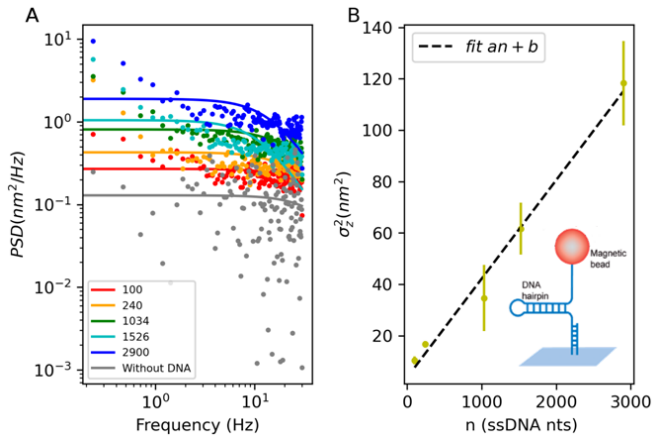


FIG. 5: (A) Power spectrum of the  $z$  position for the different lengths, as well as one power spectrum corresponding to the tracking without DNA tethered to the beads (from Fig.(2)). (B) Variance of  $z$  position for the number of open nucleotides, with a linear fit and a representation of a DNA hairpin

obtained with melted beads (Fig.2). The level of the noise when the molecule was very short was of the same order as the one obtained in the tracking noise, meaning that we are reaching the regime where Brownian and tracking noise are comparable. Note that the two experiments were not done at the same light intensity. Since assays with melted beads were done at higher light intensity, the results we measure for the shortest molecule are closer to overlap with the tracking noise results. By measuring the variance as a function of the number of open nts  $n$  (Fig.(4B)) we verified the expected lineal dependence  $\sigma_z^2 \propto n$  (Eq.(7)).

#### IV. CONCLUSIONS

In this work we have investigated and characterised the different sources of noise in MT experiments: the tracking noise, the Brownian noise and the low-frequency noise. We first characterised the tracking noise due to

the finite number of photons that arrive to the photo-detectors of the camera. Using immobilized beads we determined that the SNR increases with the frequency at which the camera takes the data  $f_s$ , with a  $\sqrt{f_s}$  rate, which is expected for a shot noise. From the power spectrum we also proved that this type of noise corresponds to a Poissonian shot noise, as the PSD was flat.

We also investigated the Brownian noise of beads tethered with DNA molecules from two different perspectives: one varying the magnetic force applied to the beads and another one varying the length of the molecular tether. The tethered DNA molecule can be seen as an over-damped pendulum that follows a Langevin dynamics. In this scenario, the PSD follows a Lorentzian function and the amplitude of the fluctuations in each direction are inversely proportional to the stiffness of the system in that direction. For the force experiments we measured and characterise the noise in  $x$  and  $z$  directions and verify that both follow the same relation with the stiffness (Eq.(2)). We also proved that the length of the molecule affects the noise, with a lineal dependence on the number of open nts.

Comparing all results, we can conclude that the main limitation in the resolution of MT experiments with DNA tethers is the noise associated to the Brownian motion. Only for very small molecules (shorter than 100 nts) the tracking noise might become limiting. Finally, the drift due to mechanical and thermal variations can be observed in all measurements as an increase in the PSD values at low frequencies. This low-frequency noise can be partially overcome by averaging results from several immobilised beads and subtracting this average value to the signal of the bead of interest.

#### Acknowledgments

I am extremely grateful to my advisor M.Mañosas for helping me in all the aspects of the project. I would also like to thank V.Rodríguez, who has helped me enormously in the programming part. Special thanks to my family and friends for their support.

- 
- [1] Neuman, K. C., Nagy, A. (2008). Single-molecule force spectroscopy: optical tweezers, magnetic tweezers and atomic force microscopy. *Nature methods*, 5(6).
  - [2] De Vlaminc, I., Dekker, C. (2012). Recent advances in magnetic tweezers. *Annu. Rev. Biophys.*, 41(1), 453-472.
  - [3] Dulin, D., Cui, T. J., Cnossen, J., Docter, M. W., Lipfert, J., Dekker, N. H. (2015). High spatiotemporal-resolution magnetic tweezers: calibration and applications for DNA dynamics. *Biophysical journal*, 109(10), 2113-2125.
  - [4] Lionnet, T., Allemand, J. F., Revyakin, A., Strick, T. R., Saleh, O. A., Bensimon, D., Croquette, V. (2012). Single-molecule studies using magnetic traps. *Cold Spring Harbor Protocols*, 2012(1).
  - [5] Bouchiat, C., Wang, M. D., Allemand, J. F., Strick, T., Block, S. M., Croquette, V. (1999). Estimating the persistence length of a worm-like chain molecule from force-extension measurements. *Biophysical journal*, 76(1), 409-413.
  - [6] Ding, F., Cocco, S., Raj, S., Manosas, M., Nguyen, T. T. T., Spiering, M. M., ... Croquette, V. (2022). Displacement and dissociation of oligonucleotides during DNA hairpin closure under strain. *Nucleic Acids Research*, 50(21), 12082-12093.